Science and Innovation. 2014. V. 10. No. 2. P. 37—44

Miroshnichenko, S.I. and Nevgasimiy, A.A.

Teleoptic, Ltd., Research and Production Association, Kyiv

MULTI-SENSOR DIGITAL X-RAY RECEIVERS

The multi-sensor structures have been successfully used in manufacture of digital receivers. A lot of sensors forming the partial image allowed the researchers to obtain the optimal parameters of radiographic, mammographic, and fluoroscopic receivers. The paper deals with analysis of multi-sensor structure properties, substantiation of options of their implementation, and noise attenuation in X-ray receivers.

Key words: digital X-ray receivers, digital receivers, flat panels, and multi-sensor receivers.

Starting with the first X-ray receiver manufactured by *Swissray* [1] where the image was formed by four matrices of charge-coupled devices (CCDs), the multi-sensor structures have become an integral part of digital receiver techniques. The use of many sensors (Sensors Array or SA) forming partial images (Fig. 1) ensures relatively inexpensive X-ray, mammographic, and fluoroscopic receivers with optimal parameters. Nevertheless, the share of SA-structures in the world market is relatively small. It does not exceed 10%. This is because of noises appearing in multi-channel structures which cannot always be effectively removed in receivers.

The receivers on SA-structures were developed in Ukraine in the late 1990s. On the basis of them a new type of digital X-ray receiver structures was designed. Chronologically, the first receivers were based on the extra-large CCDs matrices. These receivers are simple, but have a large size, weight, and quite low sensitivity (Table 1, col. 1). The last factor is caused by complexity of manufacturing the aperture lenses for large CCD matrices. The resolution was low and amounted to 2.5—3 lp /mm.

As compared with the first generation receivers on CCD matrices having the above mentioned shortcomings the creation of flat panel detectors (FPD) based on amorphous silicon and receiving layer of CsI (developed by *Trixell*, a subsidiary of *Siemens*, *Phillips*, and *Thompson*) seemed to be a perfect solution. Another promising project supported by the U.S. government was to create a flat panel based on amorphous silicon and amorphous selenium. Thus, the flat panels became the second pillar in designing the digital X-ray receivers.

The development of flat panels (Table 1, col. 2 and 3) requires investments of 100 million U.S. dollars for each project. The panels had a resolution of 3.5—3.6 lp/mm and a high detection quantum efficiency DQE = 0.4—0.7 at low frequencies. Unfortunately, both projects faced a mismatch between integrated technique capacity (several hundred thousand items per year) and relatively small orders. This resulted in a high cost and a low pace of progress in panel design. In addition to the above said, the significant internal noises, defective areas, and degradability peculiar to amorphous materials complicated the use of panels. Despite these shortcomings, since 2005, the digital receivers based on flat panels have been leading the pack in sales on the world market. In 1997, a prototype model of X-ray receiver (Fig. 2) with a field of 43 × 43 cm and a resolution 7 lp/mm (which was doubled as com-

© MIROSHNICHENKO, S.I. AND NEVGASIMIY, A.A., 2014

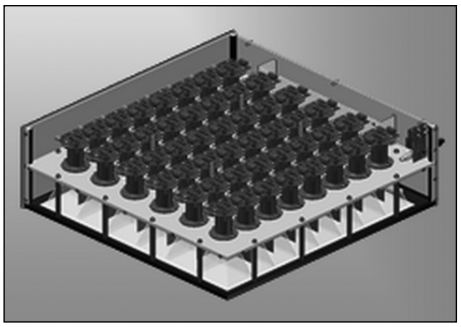

Fig. 1. Layer structure of SA-receiver from top to bottom: field of sensors, lenses, bearing plate, blinds, receiving screen, and deck

pared with the flat panels) was demonstrated at the RSNA exhibition (Chicago, USA) by *Cares Built* (USA). The 99 matrix SA-structure designed by *Teleoptic* (Kyiv) upon request of *Cares Built* (USA) ensured the maximization of receiver parameters. The receiver was the first device based on auto-calibration by overlapping areas of sensor fields of view. In this technique the received image contains all the points of original X-ray image, with the boundaries of partial images not being visually detectable. In February 2002, the FDA authorized the use of multi-sensor detectors in the U.S. market [1]. This meant that the third pillar of digital X-ray detector design, the use of SA-structures with self-calibration, was officially recognized as an effective technique.

The mammographic receiver manufactured by *Bennett* showed the best performance. The receiver consisted of tight-fitting fiber optic inhomogeneous cables (focons) the larger ends of which were fixed to the receiving screen, while the CCD matrices were glued on the smaller ones. The receiver resolution was 12 lp/mm. This has been still the best result for digital mammographic detectors.

The main disadvantages of SA-structure were as follows: partial loss of original X-ray image on the borders of focon fields and absence of overlapping matrix fields, which excluded self-calibration. As a result of sensor temperature drifts their transmission coefficients changed. Consequently, a «chessboard» noise appeared on image. The failure of this SA-structure led to the idea of complexity and inefficiency of algorithms for partial image stitching in multi-sensor structures.

Within the period from 1998 to 2004, under the severe economic and operating restrictions, *Teleoptic* was developing the multi-sensor technique for digital X-ray receivers with self-calibration. Despite this, in 2004, the company's sales of SA- based receivers made up about 4%; whereas in 2012, they accounted for about 5% of the world market of digital receivers of all types.

In 2000—2006, the corporations continued to develop the receivers on extra-large CCDs. Using the *Kodak* CCD matrix designed for the Hubble space telescope the Canadian *IDC* Ltd. released its *X-plorer* 1700 receiver with a resolution of 4.6 lp/mm (Table 1, col. 4). The receiver had a large size (optical path length was about 1 m) and a

Table 1

Parameters of receivers of three designs

Receiver	Digital AddOn — Buckey	Pixium 4600	Direct Ray	X-plorer 1700	Iona-R-4343
Manufacturer	Swissray	Trixell	Direct Radiology	IDC Ltd	Телеоптик
Detection technique	4 CCD matrixes	CsJ + a Si	a Se + a Si	CCD matrix	48 HAD sensors
Field size, mm	350 × 430	426 × 432	350 × 430	430 × 430	430 × 430
Resolution, lp/mm	3.0	3.5	3.6	4.6	4.6
DQE(0)	0.3*	0.7	0.45	0.35*	0.4*
Time of processing, s	10	4	12	15	10
Archive	DICOM-3	DICOM-3	DICOM-3	DICOM-3	DICOM-3

Note: * Value calculated by formula (1).

weight of about 75 kg. Nevertheless, high quality of image was a passport to market.

Since 2005, in the global market, there appeared new multi-sensor radiographic detectors with self-calibration: *NAOMI* 192-sensor panel (Fig. 3) manufactured by *RF System lab*. [2] and *Tradix*-100p 9-sensor receiver manufactured by *Star V-Ray Co*., Ltd., Korea. Year by year, the multi-sensor receivers with self-calibration are gaining more popularity due to their high engineering, economic, and performance parameters. In 2010, *Teleoptic* completed the Euro-certification and started to sell *Iona-R-4343* SA-receiver (Table 1, col. 5). As compared with *X-plorer* 1700 receiver, it has the same resolution (4.6 lp/mm), but a three times less thickness (22 cm) and a weight less than 25 kg. The receiver is easy to operate and to repair. This makes it popular in the markets of Central and Eastern Europe.

QUANTUM DETECTION EFFICIENCY

The different types of digital X-ray receivers can be compared by calculating the efficiency of optoelectronic path. For this purpose one can use a well-known formula for detection quantum efficiency at a low frequency [3, 4]:

$$Q_u = \frac{k_e}{1+\frac{1}{k_P k_O}+\frac{1}{k_P k_O QE_{PZS}}+\frac{N_a^2}{(k_P k_O QE_{PZS})^2 k_e N_i}}, \quad (1)$$

where k_e is coefficient of capture of X-ray photons by receiving screen; k_p is coefficient of transformation of the X-ray photons into those visible on screen; k_O is coefficient of optical path transfer; QE_{PZS} is quantum efficiency of photo-receiving sensor; N_a is number of noise electrons when reading the pixel; N_i is number of X-ray photons per pixel on screen.

If case of ideal optoelectronic path, when k_O = 1, QE_{PZS} =1, and N_a = 0, the equation (1) is transformed as:

$$DQE_{ID}(0) = \frac{k_e}{1+2/k_P}.$$

Usually, inasmuch as the coefficient of transformation of X-ray photons into those visible on receiving screen (k_p) exceeds 1000, one can assume that $DQE_{ID}(0) = k_e$ with a sufficient accuracy. The receiver relative quantum efficiency of detection which characterizes the quality of its optoelectronic channel can be represented as:

$$Q_u = \frac{DQE_{PZS}(0)}{DQE_{ID}(0)} = \frac{1}{1+\frac{1}{k_P k_O}+\frac{1}{k_P k_O QE_{PZS}}+\frac{N_a^2}{(k_P k_O QE_{PZS})^2 N_i}}. \quad (2)$$

Table 2 shows the typical parameters for the known schemes of matrix digital receiver structures: size of pixel array is $N_x N_y$, size of pixel is L_{pix}, lens aperture F, as well as QE_{PZS} and N_a.

Fig. 2. 99-matrix SA-structure receiver, 1997

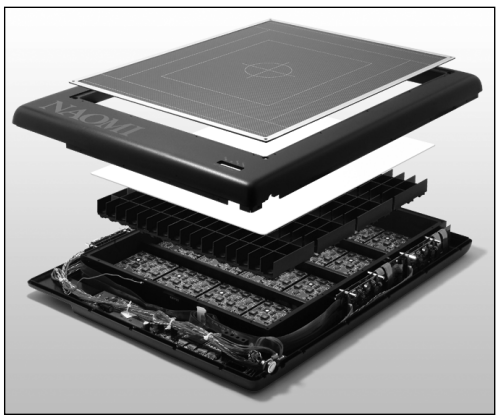

Fig. 3. Layer structure of *NAOMI* 192-sensor panel, from top to bottom: deck, receiving screen, lens hoods (blinds), and field of sensors with electronics

For the calculations the parameters were adjusted to the field receiver size 381 × 381 mm (15″ × × 15″) and to the dose in entrance plane D = 1 mR. The quality of optoelectronic paths in Table 2 is determined by the receiver resolution R and relative quantum efficiency of detection Q_u.

The results of calculations have showed that the relative quantum efficiency of detection Q_u of FPD optoelectronic path is higher than that of the structures with lenses. At the end of the 1990s, this fact caused overestimated prospects for application of flat panel receivers. Unlike the FPD receivers the medium-sized (less than 30 mm) CCD-matrices gives the structures with a low relative quantum efficiency of detection Q_u = 0.25—0.26 (Table 2, lines 1 and 2). This leads to a 4-time excess of radiation exposure dose per patient as compared with the ideal receiver. The use of large matrix with a side of about 40 mm (Table 2, line 3) results in doubled Q_u parameter.

The 4-matrix structure of CCD-matrix receiver with large pixels has a raised relative quantum efficiency of detection Q_u = 0.54 (Table 2, line 4). Among the disadvantages of this receiver there are a low resolution and a high price.

As regards the SA technique which is developing in Ukraine, in order to raise resolution and parameter Q_u it is necessary to increase the quantity of matrices and their area. So, for a field of 381 × × 381 mm a grid of 48 standard 1/3″ sensors (Table 2, line 5) with a pixel size of 10 × 10 μm gives resolution of 3.8 lp/mm at Q_u = 0.54. This model has a high feasibility and effectiveness [5] and currently is used in 20 world countries. A further increase in resolution up to 4.3 lp/mm in standard 70-sensor models (Table 2, line 7) is accompanied by an increase in relative quantum efficiency of detection up to Q_u = 0.6. The resolution of this 70-sensor model is higher than that of the flat panel, with the former having a slightly less relative quantum efficiency of detection than the latter.

The maximum resolution for X-ray receivers was reached for 48-sensor structure (Table 2, line 6) by using 1/2″ sensors whose area was twice larger. The total digital matrix 4500 × 4600 is realized with relative quantum efficiency of detection Q_u = 0.48 which is higher than that of the same receiver on one CCD matrix (Table 2, line 4). The use of 1/2″ sensor for 70-sensor model allows for realization of receivers with mammographic resolution (R = 7.3 lp/mm) and high relative quantum efficiency detection, on the one hand. On the other hand, there is an opportunity to create extra-sensitive receivers. When forming the virtual pixel having a size of 17 microns using 2-fold binning in sensors (Table 2, line 8) the receiver with a resolution of 4.0 lp/mm and a relative quantum efficiency of 0.82 was obtained [6]. The sensitivity of this receiver is equivalent to that of X-ray image intensifier and converter tube. Combining the above mentioned receiver with a micro-focus X-ray generator [7] the complex for neonatology has been made. With its help the possibility to observe a phantom with 1% contrast at a dose of 0.2 mR has been confirmed experimentally. This is much more sensitive than the X-ray film.

Using fourfold binning in the 70-sensor model one can observe a phantom with 2% contrast at a dose rate of 0.05 mR/s and get a resolution of 2.0 lp/mm in the field of receiver having a size of 381 × 381 mm (539 mm diagonal). This dynamic receiver replaces the X-ray image intensifier on X-ray image intensifier and converter tube.

MULTICHANNEL NOISE ELIMINATION

In 1996, a method for designing high-resolution X-ray TV system was proposed [8]. It allows for the use of optical path on the basis of array/screen combination of optical channels consisting of lenses and sensors. To solve correctly the full image recovery problem using the partial images it is necessary to know the correlations on the boundaries of partial fields of view. In this approach, the information about correlation relationships is provided by overlapping the partial fields of view. In addition, each image can be used to calibrate the system.

The receivers with self-calibration are distinguished by resistance to changes in external conditions and sensor parameter drifts. They do not require recalibration for many years. Conversely,

if the receiver design does not allow for the direct measurement of correlation between the signals on boundaries of partial images, especially, if a part of full image pixels is lost on the boundaries, the problem of full image reconstruction by partial components becomes incorrect. There is a risk of image distortion during stitching.

The shortcomings of X-ray image reconstruction algorithms include (a) a low signal / noise ratio as a result of compliance with the requirements for reduction of dose per patient and (b) the presence of X-ray noise of radiation source. They significantly hamper the effective decision of ill-defined problem.

IMAGE STITCHING ON THE BASIS OF CALIBRATION TEST

The model of image distortions in SA-systems can be represented by two consecutive links. *The first one* describes the spatial distortion of partial images $G_s\{X, Y, k\}$; *the second one* deals with the elementwise effects associated with changes in signal brightness intensity $G_B\{X, Y, k, t, B\}$.

General expression for the distortion operator is as follows:

$$G\{X, Y, k\} = Gs\{X, Y, k\}\, G_B\{X, Y, k, t, B\}, \quad (3)$$

where X, Y are spatial coordinates; t is time; k is number of optical channel; and B is intensity of luminance signal.

The reproduction means to find an inverse transformation which describes the elimination of distortions (3) appearing during the image formation:

$$B'(X, Y, t) = G^{-1}\{X, Y, t, k, B(X, Y, t, k)\}, \quad (4)$$

where $B'(X, Y, t)$ is reconstructed image.

In this case the aim is to obtain the reconstructed image suitable for further analysis by operator (radiologist).

The image distortions can be divided into a) *the time-determined* and b) *the time dependent* ones. The first type includes the spatial (geometric) and elementwise brightness distortion describing the light characteristics of individual pixels of optical channel.

The spatial distortions are caused by the following factors: geometric lens distortion, nonperpendicularity of the lens optical axis to the sensor plane, and geometric heterogeneity of receiving screen plane (light source). To find the inverse operator $G_s^{-1}\{X, Y, k\}$ it is proposed to use an a priori simulation method based on distortion analysis of test objects [6]. A linear grid was used as one of the first test objects (Fig. 4) where each line segment within the test is observed at least by two adjacent sensors. The correction procedure provides for the restoration of grid original rectangular shape.

The transformation of image coordinates (correction) is performed horizontally in accordance

Table 2

Parameters of receiver optical and electronic paths

Line	Receiver structure	$N_x N_y$	L_{pix}, μm F	F	OE_{PZS}	N_a	R, lp/mm	Q_u
1	1 CCD	2048 × 2048	14	1.1	0.3	25	2.7	0.25
2	1 CCD	3000 × 3000	10	1.1	0.3	25	3.9	0.26
3	1 CCD	4000 × 4000	10	0.95	0.35	25	4.6	0.45
4	4 CCD	2200 × 2200	25	1.1	0.3	25	3.0	0.54
5	6 × 8 SA (1/3″)	2900 × 2900	10	0.8	0.65	25	3.8	0.54
6	6 × 8 SA (1/2″)	4500 × 4600	9	0.8	0.65	25	4.6	0.48
7	7 × 10 SA (1/3″)	3300 × 3300	10	0.8	0.65	25	4.3	0.60
8	7 × 10 SA (1/2″)	3100 × 3100	17	0.8	0.65	25	4.0	0.82
9	FPD(aCsJ-aSi)	2700 × 2700	140	0	0.1	1000	3.6	0.95

with the formula:

$$C' = C'_S + C\frac{C'_e - C'_S}{C_e - C_S}, \qquad (5)$$

where C is coordinates X (Y) of pixels in the input image; C' is coordinates of pixel in the output corrected image. The vertical correction is performed in a similar way.

The quality of correction of geometric distortions depends on accuracy of determining the coordinates of test object elements (grid lines or points). To improve the accuracy of restoration of geometric distortion operator the polynomial approximation of center coordinates of grid lines or points is used, with the coordinates being computed by the algorithm for finding the center of mass.

The second type of time-determined image distortions G_B {X, Y, k, B} affects their brightness. It is caused by the fact that the lens transmittance coefficients throughout field, the light sensor characteristics, and the constant component of signal amplification factors at matrix output are not identical.

The problem of restoration of operator G_B {X, Y, k, B} is solved by analyzing a series of images of pure field. In this case the test images are images obtained for different values of X-ray dose in the absence of objects within the field of view.

Usually, the CCD brightness is quite well described by polynomial of the 4th order (up to 1 graduation of gray for 12-bit signal representation). At each point of image, the brightness of test image assigns an approximation knot.

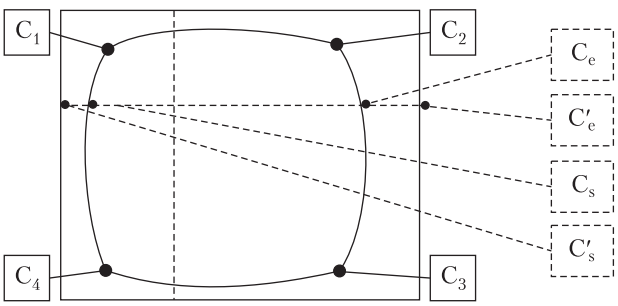

Fig. 4. Distortions of grid cell image

The brightness distortion of image is corrected in accordance with the formula:

$$B_{out}(X, Y) = B_{in}(X, Y) - C_{F1}(X, Y, n)\, C_{F2}(X, Y, n) + B_{ref}(n), \qquad (6)$$

where C_{F1} is deviation of the n-th test; C_{F2} is slope of the n-th test curve; n is test number; $B_{ref}(n)$ is reference brightness for correction of the n-th test; B_{in} (X, Y) is input brightness; B_{out} (X, Y) is output brightness.

The sensor field correction procedure is implemented as follows: the reference point is chosen based on the maximum brightness of test object images. The brightness transformation is reduced to «adjustment» of test image brightness to the reference point. The input brightness of each sensor is recalculated by formula (6) to form an equally bright field for each test.

SELF-CALIBRATION

The above procedure for image brightness correction based on calibration tests is correct provided the non-identical transmission coefficients of lens throughout field, light sensor characteristics, and signal amplification coefficients at matrix output do not change over time. Unfortunately, this is not the case in practice. For the current image the form of operator characterizing the time variability of signal parameters of optical channels can be restored on the basis of a posteriori modeling through analyzing the parameters of images of adjacent optical channels in the overlapping areas [6]. The distortion correction parameters are calculated by solving a system of linear equations comprising the estimated statistical characteristics of image in overlapping areas.

The overlapping areas make it possible to reconstruct the entire image of the partial images reconstructed at the exit of optical channels and to eliminate the function discontinuities at the interface of partial images. For these purposes, the local spatial filtering within the overlapping areas is used. The brightness values at the same points of overlapping area observed in different channels are equalized. As a result, the images in

adjacent channels smoothly blend without apparent discontinuity at the boundaries.

The computing process is realized in accordance with the procedure described above. The error of geometric distortion correction is typically less than 0.25 pixels, and the error of brightness correction does not exceed 0.1—0.5%, which makes the image borders in neighboring channels visually unobservable. The processing rate is 5 million pixels per second. The correction of one X-ray image on serial personal computer lasts 2—3 seconds.

SERVICE INSTRUCTIONS

The modular design and self-calibration make multi-sensor receivers suitable for operation in extremely difficult conditions. Hereinafter we explain this by the example of receivers operating in digital systems for chest screening radiography (digital fluorography).

The receivers of mobile screening X-ray machines undergo a considerable mechanical stress while being carried to the place of screening, as well as are exposed to large changes in temperature, from –45 to +50 °C during idle periods on weekends and holidays.

As for the digital screening systems, the correct operation of receiver and computer system usually ensures the stability and reliability of entire X-ray complex. In this regard, in addition to high quality of X-ray images it is necessary to ensure a high reliability of receiver in a wide range of external mechanical and climatic effects.

The appropriate quality of X-ray images generated by devices for chest screening is usually provided by the following parameters: image size is, at least, 380 × 380 mm; resolution ranges from 2.5 to 4.0 lp /mm; dynamic range is 250; contrast threshold is 1% for the doses up to 1 mR maximally or 2% for the doses up to 0.4 mR maximally.

The reliability of digital X-ray machine is defined by manufacturer warranty of, at least, 18 months from date of shipment, including storage of 6 months maximally. In this case, it is desirable to have a mean time to failure (MTBF) of, at least, 1 year.

Taking into consideration the fact that the digital fluorographer has five major systems (digital receiver, computer complex, stand-mounted electromechanical part, X-ray source, and X-ray generator), each of them should have a MTBF of, at least, five years, which is typical for the multi-sensor receivers of modular design manufactured by *Teleoptic*.

Teleoptic gives a 5-year warranty for receivers. During the 1st year, the company undertakes to ensure the repair of receivers by its own service engineers. Over the next four years, the company supplies free components for replacement, with the regional service engineers making replacement and repair.

The most important issue related to operation of digital receivers is maintainability and cost of accessories. In this regard the receivers of modular design have a significant advantage. They allow for quick replacement of modules and have 100% maintainability, i.e. any receiver failure can be removed by service engineer at the location of X-ray system during a day, through replacing modular elements. The price for module should not exceed 2—3 % of the cost of receiver components or 1—2% of the receiver cost. Accordingly, the receiver must comprise 30—50 modules, with price of each not exceeding USD 100—300. For the described reliability parameters the receiver service life should be, at least, 12 years.

Thus, the receiver of digital X-ray machine should have the following technical characteristics:

- Factory warranty for digital receiver: 5 years;
- The receiver should contain 30—50 standard modules (video units) of 3—4 types maximally;
- The receiver design must provide a 100% on-site maintainability by regional service engineer;
- Price of each module should not exceed 1—2% of receiver cost;
- The receiver service life should be, at least, 12 years (with supply of component modules guaranteed by manufacturer).

CONCLUSIONS

An original approach to the creation of digital X-ray receivers designed in Ukraine has many advantages which allow us to create the Ukrainian high-tech medical products competitive in the world market.

REFERENCES

1. Palasio, M.: Shart Smart Digital Radiology. *Advance for Imaging and Oncology*, 80—81 (2002).
2. www.rfsystemlab.com
3. Maidment, A. and Yaffe, M.: Analysis of the Spatial-Frequencydependent DQE of Optically Coupled Digital Mammography Detectors. *Medical Physics,* 21 (6), 721—729 (1994).
4. Liu, Hong, Karellas, A., and Harris, L.: Methods to Calculate the Lens Efficiency in Optically Coupled CCD X-Ray Imaging Systems. *Medical Physics,* 21 (7), 1193—1195 (1994).
5. www.teleoptic-pra.com
6. Miroshnichenko, S.I., and Nevgasimiy, A.A.: Theory and Technique of Multi-Sensor Digital X-Ray Receivers. *Biotechnosphere*, 4 (10), 24—29, (2010) (in Russian).
7. Vasiliev, A.Yu. and Patrakhov, N.N.: Phase Contrast of Images in Micro-Focus X-Ray .Radiography. *Materials of the Neva Radiological Forum*, 2009, 109—111 (2009) (in Russian).
8. Miroshnichenko, S.I., Nevgasimiy, A.A., et.al: High-Resolution TV-System. Description of Invention. PCT/UA 13.11.1996. Bulletin, 8 (1999) (in Russian).

С.І. Мірошниченко, О.А. Невгасимий

БАГАТОСЕНСОРНІ ЦИФРОВІ РЕНТГЕНІВСЬКІ ПРИЙМАЧІ

Багатосенсорні конструкції з успіхом використовуються при виготовленні цифрових приймачів. Застосування великої кількості сенсорів, формуючих часткове (парціальне) зображення, дало змогу отримати оптимальні параметри рентгенографічних, мамографічних та рентгеноскопічних приймачів. В даній статті проведено аналіз властивостей багатосенсорних структур, обґрунтування варіантів їх реалізації та пошук шляхів ослаблення перешкод в рентгенографічних приймачах.

Ключові слова: рентгенівські цифрові приймачі, цифрові приймачі, плоскі панелі, багатосенсорні приймачі.

С.И. Мирошниченко, А.А. Невгасимый

МНОГОСЕНСОРНЫЕ ЦИФРОВЫЕ РЕНТГЕНОВСКИЕ ПРИЕМНИКИ

Многосенсорные конструкции прочно вошли в технику цифровых приемников. Использование большого количества сенсоров, формирующих частичное (парциальное) изображение, дало возможность получить оптимальные параметры рентгенографических, маммографических и рентгеноскопических приемников. В данной статье проведен анализ свойств многосенсорных структур, обоснование вариантов их реализации и поиск путей подавления помех в рентгенографических приемниках.

Ключевые слова: рентгеновские цифровые приемники, цифровые приемники, плоские панели, многосенсорные приемники.

Received 25.12.13